

DEDICATED TO
MY PARENTS

“If we knew what it was we were doing, it would not be called research, would it?”

— Albert Einstein

Declaration

I declare that the thesis entitled “**Selected Underutilized Fruits of Northeast India for Overall Health Improvement of Humankind.**” has been prepared by me under the supervision of Prof. Arnab Sen, Department of Botany, University of North Bengal. No part of the thesis has previously formed the basis for the award of any degree or fellowship.

Swarnendra Banerjee

[Swarnendra Banerjee]

Department of Botany,
University of North Bengal
RajaRammohunpur,
Siliguri-734013



ACCREDITED BY NAAC WITH GRADE B++

UNIVERSITY OF NORTH BENGAL

Department of Botany

RajaRammohunpur Siliguri 734013 West Bengal INDIA Phone: +91 353 2699118 FAX: +91 353 2699001

Visit us at:



www.nbu.ac.in

CERTIFICATE OF SUPERVISOR

I certify that Mr. Swarnendra Banerjee has prepared the thesis entitled "SELECTED UNDERUTILIZED FRUITS OF NORTH EAST INDIA FOR OVERALL HEALTH IMPROVEMENT OF HUMANKIND", for the award of Ph.D. degree of the University of North Bengal, under my supervision. He has carried out the work at the Department of Botany, University of North Bengal. I may further declare that the results incorporated in this thesis have not been submitted for any other degree elsewhere.

[Prof. Arnab Sen]

Supervisor

Department of Botany

University of North Bengal

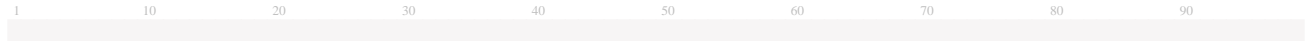
Raja Rammohunpur, Siliguri-734013

Prof. Arnab Sen
Department of Botany
University of North Bengal

Submission Information

Author Name	Swarnendra Banerjee
Title	Selected Underutilized fruits of Northeast India for overall health improvement of humankind
Paper/Submission ID	1354967
Submitted by	nbuplg@nbu.ac.in
Submission Date	2024-01-22 16:02:55
Total Pages	271
Document type	Thesis

Result Information

Similarity **0 %**

Exclude Information

Quotes	Excluded
References/Bibliography	Excluded
Sources: Less than 14 Words %	Excluded
Excluded Source	4 %
Excluded Phrases	Not Excluded

Database Selection

Language	English
Student Papers	Yes
Journals & publishers	Yes
Internet or Web	Yes
Institution Repository	Yes

A Unique QR Code use to View/Download/Share Pdf File

Swarnendra Banerjee


Prof. Arnab Sen
Department of Botany
University of North Bengal

UNIVERSITY OF NORTH BENGAL

ACCREDITED BY N A A C

DEPARTMENT OF BOTANY



समानो मन्त्रः समितिः समानी

RAJA RAMMOHUNPUR, P.O. NORTH BENGAL UNIVERSITY, DIST. DARJEELING, WEST BENGAL, INDIA, PIN - 734 013

+91 353 2776337

+91 353 2699001

botany@nbu.ac.in

www.nbu.ac.in

DRC CERTIFICATE

It is certified that the work contained in the thesis titled “SELECTED UNDERUTILIZED FRUITS OF NORTHEAST INDIA FOR OVERALL HEALTH IMPROVEMENT OF HUMANKIND” by “Mr. Swarnendra Banerjee” has been carried out following University guideline and it has been approved by the members present in the meeting of the Departmental Research Committee in Botany for processing by the Board of Research Studies.

Approved

Date: 30.01.2024

Prof. Arnab Sen

AS
Prof. Arnab Sen
Department of Botany
University of North Bengal

Name and Signature of DRC (Member)

Prof. Subhas Chandra Roy

SC
30/1/24

Name and Signature of DRC (Member)

Prof. (Dr.) S. C. Roy
Department of Botany
University of North Bengal

Prof. Monoranjan Chowdhury

MS

Dr. Monoranjan Chowdhury
Professor

Name and Signature of DRC (Member)

Department of Botany
University of North Bengal

Dr. Swarnendu Roy

SR

Name and Signature of DRC (Member)

Dr. Swarnendu Roy
Assistant Professor
University of North Bengal
Raja Rammohunpur, Pin-734013

Name of the Chairperson of DRC:

Prof. Aniruddha Saha

Full signature of the Chairperson:

Aniruddha Saha

Head
Department of Botany
University of North Bengal
Department of Botany
North Bengal University

Acknowledgement

I would like to express my heartfelt gratitude to my supervisor, Prof. Arnab Sen, for his constant guidance, encouragement, and support at every step of my work. Apart from all the guidance and freedom he has given me in accomplishing this study, I also thank him for being very kind and supportive throughout my PhD journey. His immense knowledge and plentiful experience have encouraged me throughout the course of my research.

I am indebted to Prof. A. Saha, Head of the Department of Botany, University of North Bengal. I am also indebted to Prof. S.C. Roy, Prof. M. Chowdhury, Dr. S. Roy, and Dr. P. Mathur for their guidance.

I am grateful to CSIR, Government of India, for providing the fellowship to conduct my research. I am also thankful to the Department of Botany's coordinator UGC (SAP) DRS-III and DST FIST (SANC. No. SR/FST/LS-1/2021/900)

for providing the necessary instrumental facilities.

I am thankful to my lab mates for creating an amicable working atmosphere and always being happy to help nature. I am very thankful to all the teaching staff of our department for the administrative help and technical assistance during this work. I would like to thank IIT Bombay, Jawaharlal Nehru University, and IISER Kolkata for the instrument facilities that aid my research work. I also thank USIC, University of North Bengal, for the liquid nitrogen supply.

I am grateful to Dr. Pallab Kar and Dr. Bedabrata Saha for their encouragement, unlimited enthusiasm, and inspiring discussions. His constructive feedback and advice provided the right direction for completing this thesis's work. I thank my collaborators, Sourik Mandal, Jarzis Islam, Anipa Saha,

Usashi Shome, and Rajarshi Sarkar, for their analysis and thoughtful discussions.

I am forever grateful to my parents and family members, especially my elder sister for her constant support and love.

I take this opportunity to thank my close friends for their persistent support and strong faith in my abilities, which has helped me to reach this stage.

Swarnendra Banerjee

[Swarnendra Banerjee]

Preface

A study examining 14 underutilized fruits from northeast India found that four fruit samples exhibited higher free radical scavenging activity. These fruits, *Elaeagnus pyriformis*, *Baccurea ramiflora*, *Phyllanthus acidus*, and *Prunus bracteopadus*, were selected for further examination. *In vitro*, antioxidant assays showed that fruit extracts protect cells and cellular organelles from reactive oxygen species (ROS) during stressful conditions. The fruit samples also showed higher antimicrobial activity against gram-positive and gram-negative bacteria than standard, suggesting they can be used as an herbal remedy for microorganism-related disorders. The fruit extracts also showed cytotoxic effects on the adenocarcinoma cell line in a dose-dependent manner. GC-MS analysis revealed that the fruits were rich in long-chain fatty acids and sterols,

which benefit human health. The study suggests that these fruit extracts could be used in the food and pharmaceutical industries. The study also found that *Elaeagnus pyriformis* fruit demonstrated protection against testicular oxidative stress and improved lipid metabolism in rats. Fruit extracts rich in polyphenols, including anthocyanins, phenolic acids, flavonoids, and flavanols, have been found to have beneficial effects on human health. These bioactive compounds, including antioxidant, anticancer, anti-inflammatory, and antimicrobial activity, have the potential for further use in the food and pharmaceutical industries. *In vitro* and *in silico* molecular docking analysis showed that these bio compounds could inhibit disease-related proteins, potentially leading to new drug discovery. The study also found that *Elaeagnus pyriformis* fruit

protected against testicular oxidative injury and improved lipid metabolism. Oleaster wine, a traditional wine made from underutilized fruits like silverberry, has been found to have anti-cancer effects and antioxidant properties. The wine's microbial community showed anti-cancerous solid activity. Oleaster has gained prominence both culturally and commercially. A promising drug discovery area is synthesizing biocompatible plant-mediated fusion of metal nanoparticles, which could be used as green reducing and capping agents for nanoparticle creation using *Elaeagnus* fruit extract. The study explores the potential of nanoparticles in treating oxidative stress-related illnesses and microbial infections. It also investigates the cytotoxic and anticancer properties of AgNPs, which were synthesized using BR fruit juice. The green synthesis approach suggests that nanoparticle-based cancer treatment could be beneficial. The study also investigates the benefits of

P. acidus nanoparticles (PANPs) for treating renal dysfunction and damage. The results show that PANPs enhance glomerular structure, reduce serum creatinine and urea levels, and promote growth in body weight. The study also highlights the effectiveness of nano-priming with ZnONPs in minimizing the impacts of As-stress in black grams. The study also highlights the potential of using biogenic ZnONPs in nano-remediation to lessen As-induced genotoxicity in *Pisum sativum*. The study suggests that nanoparticles can be directly employed in irrigation systems, particularly drip irrigation systems, for targeted distribution into the rhizosphere. However, the environmental dangers posed by NPs must be thoroughly investigated.

Swarnendra Banerjee

[Swarnendra Banerjee]

List of Figures

	Page #
Figure 1.1. Some common polyphenols of Fruits	9
Figure 2.1 Distribution of underutilized fruit species in different parts of the world	20
Figure 3.1 Datasheet used during the collection of Fruits.	42
Figure 3.2 Collected underutilized fruits during survey	43
Figure 4.1 <i>In vitro</i> ROS scavenging activity of EP: <i>Elaeagnus pyriformis</i> , BR: <i>Baccaurea ramiflora</i> , PA: <i>Phyllanthus acidus</i> , PN: <i>Prunus nepalensis</i> (A) DPPH (B) Hydrogen Peroxide, (C) Hydroxide radical (D) Nitric oxide (F) Hypochlorous acid (G) Total antioxidant.	113
Figure 4.2. FTIR analysis of fruit extracts (A) EP (<i>Elaeagnus pyriformis</i>), (B) BR (<i>Baccaurea ramiflora</i>), (C) PA (<i>Phyllanthus acidus</i>) and (D) PN (<i>Prunus nepalensis</i>)	118
Figure 4.3. GC-MS Chromatograms of Fruit extracts A) EP (<i>Elaeagnus pyriformis</i>), (B) BR (<i>Baccaurea ramiflora</i>), (C) PA (<i>Phyllanthus acidus</i>) and (D) PN (<i>Prunus nepalensis</i>)	120
Figure 4.4. High-Performance Liquid Chromatography (HPLC) chromatogram of <i>Elaeagnus pyriformis</i> using an LTQ Orbitrap XL mass spectrometer in a mass range from 100 to 2000 amu. (A) In Positive-ESI Ion Mode and (B) In Negative-ESI Ion Mode	127

Contd.....from the previous page.

	Page #
Figure 4.5. High-Performance Liquid Chromatography (HPLC) chromatogram of <i>Baccaurea ramiflora</i> using an LTQ Orbitrap XL mass spectrometer in a mass range from 100 to 2000 amu. (A) In Positive-ESI Ion Mode and (B) In Negative-ESI Ion Mode	128
Figure 4.6. High-Performance Liquid Chromatography (HPLC) chromatogram of <i>Phyllanthus acidus</i> using an LTQ Orbitrap XL mass spectrometer in a mass range from 100 to 2000 amu. (A) In Positive-ESI Ion Mode and (B) In Negative-ESI Ion Mode	129
Figure 4.7. High-Performance Liquid Chromatography (HPLC) chromatogram of <i>Prunus nepalensis</i> using an LTQ Orbitrap XL mass spectrometer in a mass range from 100 to 2000 amu. (A) In Positive-ESI Ion Mode and (B) In Negative-ESI Ion Mode	130
Figure 4.8. <i>In silico</i> Molecular docking (molecular surface view) between Beta sitosterol and microbial proteins (aI) 6RKW (<i>E. coli</i> DNA Gyrase complex), (aII) 4DDQ (<i>Bacillus subtilis</i> Gyrase A), (aIII) 4URM (<i>Staphylococcus aureus</i> gyrase B), (aIV) 6J90 (Gyrase B <i>Salmonella typhimurium</i>): .	131
Figure 4.9. <i>In silico</i> Molecular docking (molecular surface view) between Octadecanoic acid and microbial proteins (aI) 6RKW (<i>E. coli</i> DNA Gyrase complex), (aII) 4DDQ (<i>Bacillus subtilis</i> Gyrase A), (aIII) 4URM (<i>Staphylococcus aureus</i> gyrase B), (aIV) 6J90 (Gyrase B <i>Salmonella typhimurium</i>):	132
Figure 4.10. <i>In silico</i> Molecular docking (molecular surface view) between γ -Sitosterol and microbial proteins (aI) 6RKW (<i>E. coli</i> DNA Gyrase complex), (aII) 4DDQ (<i>Bacillus subtilis</i> Gyrase A), (aIII) 4URM (<i>Staphylococcus aureus</i> gyrase B), (aIV) 6J90 (Gyrase B <i>Salmonella typhimurium</i>)	133
Figure 4.11. <i>In silico</i> Molecular docking (molecular surface view) between Squalene and microbial proteins (aI) 6RKW (<i>E. coli</i> DNA Gyrase complex), (aII) 4DDQ (<i>Bacillus subtilis</i> Gyrase A), (aIII) 4URM (<i>Staphylococcus aureus</i> gyrase B), (aIV) 6J90 (Gyrase B <i>Salmonella typhimurium</i>):	134

Contd.....from the previous page.

	Page #	
Figure 4.12.	Antimicrobial activity of <i>Elaeagnus pyriformis</i> fruit extract against various pathogens (A) <i>Bacillus subtilis</i> (B) <i>Escherichia coli</i> (C) <i>Salmonella typhimurium</i> and (D) <i>Staphylococcus aureus</i> using agar well diffusion assay	139
Figure 4.13.	Antimicrobial activity of <i>Baccaurea ramiflora</i> fruit extract against various pathogens (A) <i>Bacillus subtilis</i> (B) <i>Escherichia coli</i> (C) <i>Salmonella typhimurium</i> and (D) <i>Staphylococcus aureus</i> using agar well diffusion assay	139
Figure 4.14.	Antimicrobial activity of <i>Phyllanthus acidus</i> fruit extract against various pathogens (A) <i>Bacillus subtilis</i> (B) <i>Escherichia coli</i> (C) <i>Salmonella typhimurium</i> and (D) <i>Staphylococcus aureus</i> using agar well diffusion assay	140
Figure 4.15.	Antimicrobial activity of <i>Prunus nepalensis</i> fruit extract against various pathogens (A) <i>Bacillus subtilis</i> (B) <i>Escherichia coli</i> (C) <i>Salmonella typhimurium</i> and (D) <i>Staphylococcus aureus</i> using agar well diffusion assay	140
Figure 4.16.	Cell viability (%) of ACHN human renal adeno carcinoma cell line upon the exposure of various concentrations of fruit juice for 48 h.	141
Figure 4.17.	In silico Molecular docking (molecular surface view) between MDM2 protein with (aI) quercetin, (bI) Malvidin, (cI) Ellagic acid, (dI) Rosmerinic acid.	142
Figure 4.18.	Effect of Resveratrol on (A) SOD (B) NOX (C) GSH and (D) MDA under the H ₂ O ₂ mediated stress in the testicular tissue	144
Figure 4.19.	Effect of Resveratrol on the protein content and lipid profile (A) Total protein (B) Cholesterol, and (C) Triglyceride, (D) HDL-Cholesterol of oxidative testicular injury	146
Figure 4.20.	In silico Molecular docking (molecular surface view) between NOX2 protein with Resveratrol.	149
Figure 4.21.	Histological sections of experimental testicular tissues stained with haematoxylin-eosin. Magnification = 200x	150
Figure 4.22.	Effect of resvratrol on sperm viability (using AO/PI dual staining method) under H ₂ O ₂ mediated oxidative stress.	152

Contd.....from the previous page.

	Page #
Figure 4.23. Schematic illustration represents the salvage mechanisms of resveratrol from H ₂ O ₂ -induced oxidative stress and sperm viability loss in swiss albino mice.	153
Figure 4.24. <i>In vitro</i> ROS scavenging activity of <i>Elaeagnus</i> wine (A) DPPH activity; (B) Nitric oxide; (C) Hydrogen peroxide and (D) Superoxide anion	157
Figure 4.25. GC-MS chromatogram of <i>Elaeagnus</i> wine	160
Figure 4.26. Molecular docking analysis of Bcl-XL protein with (A) Carnegine and (B) limonen-6-ol pivalate and their interacting amino acids.	161
Figure 4.27. Graphical presentation of cell viability (%) of (A) MCF7 (B) MDA-MB-231 (C) RAW cell line upon exposure to different concentrations of <i>Elaeagnus</i> wine for 48 h.	162
Figure 4.28. Analyzing the receiver operating characteristic (ROC) of an <i>Elaeagnus</i> wine sample	163
Figure 4.29. The wine sample's rarefaction curve	164
Figure 4.30. Schematic representation showing the free radical generation followed by the chain of by product (ROS/RNS) and how they affect biological systems by cellular stress even leading to carcinogenesis and the role of phytochemicals of <i>Olea</i> wine helps to commence the apoptosis pathway.	168
Figure 4.31. UV-visible spectra of Ag nanoparticles made by using fruit juice from <i>Elaeagnus pyriformis</i> to reduce AgNO ₃ . A: Fruit juice from <i>Elaeagnus pyriformis</i> ; B: colour modified after adding AgNO ₃	172
Figure 4.32. (A) SEM and (B) FESEM image of silver nanoparticles produced via biosynthesis	172
Figure 4.33. (A) The elemental composition and EDX spectra of nanoparticles produced by biosynthesis and (B) XRD pattern of biogenically synthesized silver nanoparticles	173

Contd.....from the previous page.

	Page #
Figure 4.34. FTIR peaks of (A) EP fruit juice and (B) Biosynthesized AgNPs	174
Figure 4.35. In vitro ROS scavenging activity of biosynthesized AgNPs (A) DPPH activity, (B) Super oxide radical, (C) Hypochlorous acid and (D) Total antioxidant scavenging activity	175
Figure 4.36. <i>In vitro</i> ROS scavenging activity of biosynthesized AgNPs (A) Reducing power assay, (B) Nitric oxide, (C) Hydrogen peroxide and (D) Hydroxyl radical scavenging assay.	177
Figure 4.37. Antibacterial activity of biogenically synthesized AgNPs against pathogenic microbial strains (A) <i>S. aureus</i> (B) <i>B. subtilis</i> (C) <i>P. aeruginosa</i> and (D) <i>E. coli</i> applying the test for agar well diffusion.	180
Figure 4.38. Three silver nanoparticles and their target protein were studied using <i>in silico</i> docking. (aI) The binding affinity of Ag-fumarate was -6.8 kcal/mol. The distances between interacting amino acids are displayed in (aII) and (aIII). Ag-laurate (bI) showed a -6.8 kcal/ mol binding affinity. The distances between interacting amino acids have been demonstrated in (bII and (bIII).	181
Figure 4.39. <i>In silico</i> molecular docking analysis of (A) fumarate (B) laurate and (C) palmitate with Bcl-X _L protein	182
Figure 4.40. The diagram illustrates the production of free radicals, the chain of reactive oxygen species/ reactive nitrogen species (ROS/RNS) that results from oxidative stress, and their impact on biological systems. It also highlights the role of biogenically synthesised silver nanoparticles from <i>Elaeagnus pyriformis</i> fruit juice in initiating the apoptosis pathway and causing cellular stress	183
Figure 4.41. An evaluation of the cytotoxicity of different doses of silver nanoparticles was conducted on the ACHN human renal adenocarcinoma cell line after a 24-hour exposure	184

Contd.....from the previous page.

	Page #
Figure 4.42. <i>In silico</i> Molecular docking analysis of (A) Silver laurate (B) silver palmitate and (C) silver fumarate with ABC transporter protein (6M96)	185
Figure 4.43. <i>In silico</i> molecular docking analysis of (A) laurate (B) palmitate and (C) fumarate with ABC transporter protein (6M96)	186
Figure 4.44. Illustration depicting how AgNPs interfere with cancer cells' regular processes to cause them to die by blocking ABC transporter	186
Figure 4.45. Characterization of biogenic AgNPs (A) SEM, (B) FESEM, (C) EDX, (D) XRD, (E) HRTEM and (F) DLS and Zeta potential	188
Figure 4.46. <i>In vitro</i> ROS scavenging activity of biosynthesized AgNPs (A) DPPH activity, (B) Super oxide radical, (C) Nitric oxide and (D) Hydrogen peroxide scavenging activity.	190
Figure 4.47. Antibacterial activity of biogenically synthesized AgNPs against pathogenic microbial strains (A) <i>B. subtilis</i> (B) <i>S. aureus</i> (C) <i>E. coli</i> (D) <i>P. aeruginosa</i> and (E) <i>S. typhimurium</i> applying the test for agar well diffusion.	192
Figure 4.48. MCF-7 and MDA-MB-231 cell viability (%) after 48 hours of exposure to various AgNPs concentrations. Positive control was provided by mitomycin-C.	195
Figure 4.49. (A) SEM (B) FESEM micrograph of biosynthesised AgNPs	196
Figure 4.50. (A) EDX (B) XRD images of biosynthesised AgNPs	196
Figure 4.51. <i>Phyllanthus acidus</i> fruit juice GC-MS chromatogram	198
Figure 4.52. <i>In vivo</i> antioxidant activities of <i>P. acidus</i> fruit juice and <i>P. acidus</i> nanoparticle (A) SOD activity (B) Catalase (C) GSH activity (D) MDA activity	201
Figure 4.53. The figure illustrates how Gentamicin can cause nephrotoxicity and how biosynthesised AgNPs can lessen nephrotoxicity	202

Contd.....from the previous page.

	Page #
Figure 4.54. Histology of treated and control mice's kidney tissues (A–G).	204
Figure 4.55. <i>In silico</i> molecular docking analysis of (A) Ag-hexadecanoic acid (B) Ag -octadecanoic acid with NFκβ protein	205
Figure 4.56. Molecular docking analysis of (A) Hexadecanoic acid (B) Octadecanoic acid with NFκβ protein	205
Figure 4.57. Stepwise (a-d) biogenic synthesis of zinc oxide nanoparticles (ZnONPs)	206
Figure 4.58. Zinc oxide nanoparticle (ZnONPs) characterisations	207
Figure 4.59. Impact of Zinc Oxide Nanoparticles priming on morpho-physiological characteristics in <i>Vigna mungo</i> seedlings exposed to arsenic stress	209
Figure 4.60. ZnONPs primings effects on the morpho-physiological characteristics of <i>Vigna mungo</i> plants under Arsenic (As) stress	211
Figure 4.61. Superoxide radical and cell death in <i>V. mungo</i> seedlings were detected <i>in vivo</i> using (a) NBT and (b) Evans blue staining	215
Figure 4.62. Superoxide radical and cell death was detected <i>in vivo</i> in <i>V. mungo</i> plant using (a) NBT and (b) 4x microscopic view and (c) Evans blue staining	215
Figure 4.63. Impact of increasing ZnONPs concentration under as-stress conditions on (a) Plant cell death quantification, (b) Seedling cell death quantification, (c) MDA content, and (d) H ₂ O ₂ content measurement	216
Figure 4.64. The impact of Arsenic-induced pigment degradation and ZnONPs-mediated alleviation (a) seedling chlorophyll, (b) plant chlorophyll, (c) Seedling carotenoid and (d) Plant carotenoid	218

Contd.....from the previous page.

	Page #
Figure 4.65. ZnONPs impact the following metabolite levels in <i>V. mungo</i> under stress (a) Total sugar, (b) Total protein, (c) Total phenolics, (d) Proline, and (e) GSH content	222
Figure 4.66. Impact of increasing concentration of ZnONPs on the activity of antioxidant enzymes under As-stress.(a) SOD, (b) CAT, (c) GPOX and (d) APX under As-stress.	225
Figure 4.67. PCA-generated score plots (a and b) for various treatments and factors loading plots (c and d) in <i>V. mungo</i> seedlings In <i>V. mungo</i> plants.	226
Figure 4.68. (a) Hierarchical heatmap study of several factors about treatments in <i>V. mungo</i> seedlings. (b) Hierarchical heatmap analysis of several parameters in <i>V. mungo</i> plants with treatments.	227
Figure 4.69. Comparative analysis of the many factors involved in As-toxicity and how ZnONPs mitigate in <i>V. mungo</i> .	230
Figure 4.70. Characterization of zinc oxide nanoparticles (ZnONPs) produced via biological synthesis (a-f). (g) SEM of starch grain (h) ZnONPs' <i>in-vitro</i> As-adsorption (i) <i>Pisum</i> seed germination percentage under arsenic stress (j) Variations in the number of starch grain (j) The regulation of α -amylase activity during arsenic stress.	233
Figure 4.71. ZnONPs effects on morpho-physiological parameters in stressed <i>P. sativum</i> plants (a-f).	237
Figure 4.72. The treatment of ZnONPs reduces detrimental effects of as-induced stress on <i>P. sativum</i> leaf photosynthetic activity (a-d).	238
Figure 4.73 Unsing light microscopy examination of guard cell lipid peroxidation and changes in stomatal aperture under arsenic stress and ZnONPs mediated recovery	240
Figure 4.74. Effect of ZnONPs under As-stress on: (a) Total protein (b) Total phenolics (c) Total sugar content	242

Contd.....from the previous page.

	Page #	
Figure 4.75.	Effects of increasing dosage of ZnONPs on: (a) GSH content (b) Total phytochelatin content (c) Proline content (d) MDA content (e) Leaf relative water content (f) Electrolyte leakage percentage	244
Figure 4.76.	Modulation in non-antioxidant enzymes activity by ZnONPs under As-stress: (a) TAL activity (b) PAL activity	245
Figure 4.77.	<i>In-vivo</i> histochemical detection of superoxide radical ($O_2^{\cdot-}$), hydrogen peroxide (H_2O_2), lipid peroxidation, and cell death in: (a) leaf and (b) root of <i>P. sativum</i> plants under As-stress. Semiquantitative detection of: (c) superoxide radical ($O_2^{\cdot-}$) (d) hydrogen peroxide (H_2O_2) (e) lipid peroxidation, and (f) Cell death, based on relative stain intensity (RSI) in leaves and roots. (g) Fluorometric detection of total ROS in leaf and (h) root under a fluorescence microscope using H_2DCF -DA (i) Relative Fluorescence intensity (RFI) of H_2DCF -DA stained leaves and roots.	247
Figure 4.78.	Effect of ZnONPs under As-mediated oxidative stress on: (a) pollen viability, detected by MTT staining (b) Pod morphology (c) Viable and non-viable pollen count (d) Pod number per plant (e) Pod length and (f) Seed number per plant.	253
Figure 4.79.	Fluorometric detection of genotoxic effects due to As-stress and ZnONPs mediated amelioration by: (a) Representative CLSM images showing the Changes in nuclear morphology of root cells of the treatment groups (b) Alkaline comet assay of root cell nucleus [true DAPI fluorescence color (blue) is converted to 'cyan' using ImageJ software, for better visibility of comet tails] (c) Nuclear area expansion (d) Changes in comet tail DNA percentage (e) Changes in Olive tail moment (f) Representative CLSM images of programmed cell death (PCD) in root cells (g) PCD stages of the nucleus.	255
Figure 4.80.	Isolated <i>P. sativum</i> high molecular weight DNA was quality checked by agarose gel (0.8%) electrophoresis method. Lane 'L' contains a λ -double digest molecular marker.	258

	Page #
Figure 4.81.	Genomic template stability (GTS) assessment by RAPD profiling using random primers: (a) OPA 01(b) OPA 02 (c) OPA 09 respectively. Lane ‘L’ contains a λ -double digest molecular marker. 258
Figure 4.82	(a) Arsenic stress-induced genomic variability and loss in genomic template stability (GTS) detected through RAPD analysis. Lane ‘L’ contains λ -double digest molecular marker (b) Gene expression analysis of arsenate reductase (AR), phytochelatin synthase (PCS), superoxide dismutase (SOD), catalase (CAT), glutathione reductase (GR), GIGANTIA (GI), CONSTANS (CO), and FLOWERING LOCUS T (FT) through qRT-PCR. area (c) Total arsenic and zinc content in root, shoot, and seed of <i>P. sativum</i> . (d) Root to shoot translocation factor of arsenic and zinc (e) Heatmap-based cluster analysis (f) Correlogram of considered. 259
Figure 4.83.	. Primer specificity and gene expression pattern were primarily checked by: (a) Agarose gel electrophoresis of semi-quantitative Reverse Transcriptase PCR (sqRT-PCR) products of respective genes (b) Changes in relative band intensity among the target genes after normalizing with β -Actin. 262
Figure 4.84.	Schematic illustration represents the salvage mechanisms of ZnONPs from arsenic-induced oxidative stress, genotoxicity, and yield loss in <i>Pisum sativum</i> . 263

List of Tables

	Page #
Table 1.1	Different Free radicals 5
Table 2.1.	Main centers of diversity for underutilized fruits in India. 19
Table 2.2.	Diversity of underutilized fruit crops in Northeast India. 21
Table 2.3.	Nutritive value of underutilized fruit crops of the NEH Region 22
Table 2.4.	List of underutilized fruit crops with potential uses in medicine 23
Table 3.1.	Information regarding <i>Pisum sativum</i> gene-specific primers, used in qRT-PCR analysis 105
Table 4.1.	Collection of different underutilized fruit samples 110
Table 4.2.	All fourteen underutilized fruit samples Percentage of inhibition 112
Table 4.3.	IC ₅₀ values of each fruit extract with their respective standard used in the present study 114
Table 4.4.	Total Phenol and Flavonoid content of Selected Fruit samples 116
Table 4.5.	FTIR wavenumber and Functional groups of fruit extracts 118-119
Table 4.6.	List of Biologically important phytochemicals identified in <i>Elaeagnus pyriformis</i> and <i>Baccaurea ramiflora</i> fruit juice 121
Table 4.7.	List of Biologically important phytochemicals identified in <i>Phyllanthus acidus</i> and <i>Prunus nepalensis</i> fruit juice by GC-MS analysis 122
Table 4.8.	List of compounds detected from the lyophilized sample of <i>Elaeagnus pyriformis</i> and <i>Baccaurea ramiflora</i> fruit by HR-orbitrap LC –MS 124

Contd.....from the previous page.

	Page #
Table 4.9. List of compounds detected from the lyophilized sample of <i>Phyllanthus acidus</i> and <i>Prunus nepalensis</i> fruit by HR-orbitrap LC-MS	125
Table 4.10. Molecular docking results showing compounds and their binding affinity	135
Table 4.11. Antibacterial activity of selected four fruit extracts	136
Table 4.12. Molecular docking results showing compounds and their binding affinity	143
Table 4.13. List of phytochemicals identified in <i>Elaeagnus</i> wine GC-MS analysis	159
Table 4.14. List of microbes involved in anticancer activity	166
Table 4.15. Antimicrobial activity of bio-nanomaterial (AgNO ₃ + EP) by agar well diffusion	179
Table 4.16. Antimicrobial activity of bio-nanomaterial (AgNO ₃ + BR) by agar well diffusion	193
Table 4.17. List of phytochemicals found by GC-MS analysis in the fruit juice of <i>Phyllanthus acidus</i>	198
Tale 4.18. List of phytochemicals found by GC-MS analysis in the fruit juice of <i>Phyllanthus acidus</i>	199
Table 4.19. Impact of <i>Phyllanthus acidus</i> juice and <i>Phyllanthus acidus</i> nano on treated mice's body weight.	199
Table 4.20. Impact of <i>Phyllanthus acidus</i> juice and <i>Phyllanthus acidus</i> nano on treated mice's body weight.	200
Table 4.21. A synopsis of the toxicity studies of arsenic (As) in 7 DAS Seedlings of <i>Vigna mungo</i> subjected to various treatments	210

Contd.....from the previous page.

		Page #
Table 4.22.	Zn and total arsenic (As) levels in tissues, together with associated translocation factors, in 28 Vigna mungo plants cultivated in DAS under various conditions	229
Table 4.23.	Modulation in antioxidant enzymes activity	241
Table 4.24.	RAPD profiling: sequence information of random 10-mer oligonucleotide primers, those produced reproducible polymorphic bands and genomic template stability (GTS) determination from the number of polymorphic bands of different treatment	258

List of Appendices

	Title	Page #
Appendix A	List of Publications	A1
